

# Crack-bridging force transfer of composite strengthening: a dynamic point of view

P.A. Ovigne<sup>†</sup>, M. Massenzio<sup>‡</sup>, E. Jacquelin<sup>‡</sup> and P. Hamelin<sup>‡†</sup>

*Laboratoire Mécanique Matériaux et Structures, Université Claude Bernard, 82 boulevard Niels Bohr,  
Domaine scientifique de la Doua, 69622 Villeurbanne, France*

*(Received July 26, 2002, Accepted January 30, 2003)*

**Abstract.** This study focuses on the influence of a composite external strengthening on the natural frequencies of a steel beam with open cracks. In a first step, the leading parameters associated with the effect of the composite strengthening are experimentally identified. An analytical model is developed in order to quantify the importance of the force transfer within the resin interface. In a second step, the analytical model of a cracked beam with composite external strengthening is compared to experiments.

**Key words:** natural frequencies; mode shape; crack; external strengthening; shear stress.

---

## 1. Introduction

For the past two decades, external strengthening involving composite material has appeared as an innovative technique to solve various problems associated with aging and damaging structures. The wide range of composite materials and their highly specific mechanical properties make them very attractive for this purpose (Meier, Deuring, Meier, Schwegler 1992), (Triantafillou 1998). Although numerous studies have already been carried out on the static behavior of structures with composite reinforcement, the influence of the composite on the vibration characteristics of reinforced structures has yet to be explored.

First, the composite active length associated with the force transfer within the resin joint is experimentally identified as the leading parameter associated with the effect of the composite.

After, an analytical model developed in Ovigne, Massenzio, Jacquelin, Hamelin (2002) is implemented to evaluate the natural frequencies of a cracked beam with composite strengthening. Furthermore, Täljsten's model (1997) is extended to a modal case in order to obtain shear stress mode shapes of the resin joint. These mode shapes are used to evaluate the composite active length.

Finally, the analytical modeling for both natural frequencies of the beam and shear stress mode shapes of the resin joint are experimentally validated.

---

<sup>†</sup>Ph. D.

<sup>‡</sup>Assistant Professor

<sup>‡†</sup>Professor

## 2. Effect of a composite external strengthening: experimental approach

### 2.1. Specimens

A 765 mm long steel beam with a 20×39 mm section is used for this test. Open crack state is ensured by the thickness of the notches which is about 2 mm. The composite material used for the external strengthening is made of two layers of unidirectional carbon fiber wrap impregnated with epoxy resin ( $G = 1200$  MPa). The carbon wrap characteristics are: toughness: 3400 MPa, Young modulus: 230000 MPa, weight: 200 g/m<sup>2</sup>. The longitudinal Young modulus of the composite  $E_{compo}$  is experimentally evaluated by a tensile test to be 70000 MPa.

### 2.2. Natural frequencies measurement

The natural frequencies of the beam are measured in free-free boundary conditions so as to ensure test reproducibility. The vibration tests consist of hanging the beam on elastic bonds whose stiffness is lower than the value of the beam stiffness so as to simulate free-free boundary conditions. An impact hammer (Bruel and Kjaer 8202 with a force transducer B&K 8200) is used for supplying a large frequency bandwidth impulse (0-10 kHz) on the beam. An accelerometer (Metravib 103M n°937) fixed at several positions on the beam, is used to pick up its response. The excitation and the response are analyzed by a Siglab analyzer that allows us to explore the transfer function of the beam in the frequency domain.

### 2.3. Effect of the composite on the natural frequencies of an intact beam

The natural frequencies of an intact steel beam are measured in free-free boundary conditions before and after bonding the composite (Fig. 1). Only the five first bending modes are considered in this study. The results point out that the composite has no significant influence on the natural frequencies of an intact beam (Table 1). Indeed, the composite bending stiffness and mass that are superposed to these of the beam are not high enough to modify the modal scheme.

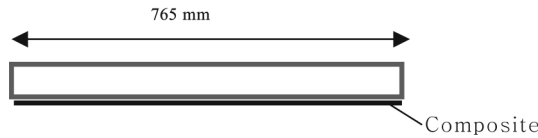


Fig. 1 Intact steel beam with composite reinforcement

Table 1 Natural frequencies (Hz) of an intact steel beam. Experiment

| Mode number | Intact beam | beam with CFRP | Increase (%) |
|-------------|-------------|----------------|--------------|
| 1           | 357         | 359            | 0.3          |
| 2           | 969         | 972            | 0.3          |
| 3           | 1853        | 1860           | 0.4          |
| 4           | 2976        | 2985           | 0.3          |
| 5           | 4292        | 4308           | 0.4          |

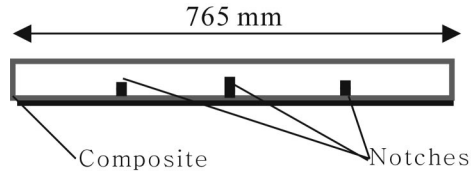


Fig. 2 Beam with 3 notches and CFRP

Table 2 Natural frequencies (Hz) of a beam with 3 notches. Experiment

| Mode number | beam without CFRP | beam with CFRP | Increase (%) |
|-------------|-------------------|----------------|--------------|
| 1           | 182               | 293            | 61           |
| 2           | 740               | 835            | 13           |
| 3           | 1109              | 1479           | 33           |
| 4           | 2838              | 2895           | 2            |
| 5           | 3847              | 4010           | 4            |

#### 2.4. Effect of the composite on the natural frequencies of a cracked beam

On the contrary, in presence of cracks, the influence of the composite is quite significant. The steel beam is now damaged by three notches with various lengths (20 mm 30 mm and 20 mm respectively), located at each quarter of span (Fig. 2). The natural frequencies are measured before and after composite reinforcement (Table 2).

The increase of the natural frequencies is due to composite bridging effect. The longitudinal stiffness of the composite limits relative displacements of the notch lips. Therefore, the damaged section is stiffened. The bridging force induced within the composite is transferred on each side of the fault by bonding. Then, an anchorage effect is brought into play with shearing of the resin joint.

#### 2.5. Effect of bridging force transfer on natural frequencies of a cracked beam

An experimental procedure is developed in order to determine the leading parameter associated with the bridging effect due to CFRP. It consists in reinforcing a beam only in the vicinity of a crack. The composite is progressively removed on each side by cutting and the natural frequencies are measured. This test points out the fact that the bridging effect is located in the vicinity of the fault. Indeed, the

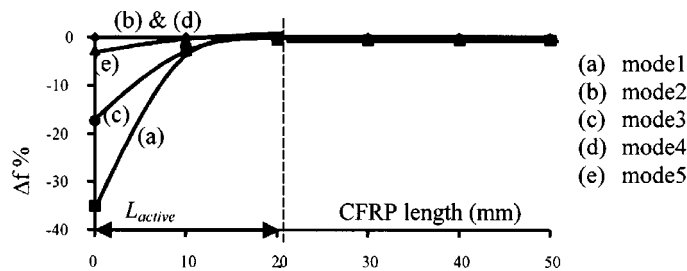


Fig. 3 Active length evaluation

natural frequencies are not affected by the composite removal outside a zone. This zone is called the active length of the composite  $L_{active}$ . On the contrary, when the length of the composite equals  $L_{active}$  the anchorage of the composite is not verified and the frequencies decrease (Fig. 3). As expected, the natural frequencies associated with the even modes are not affected by a midspan notch.  $L_{active}$  is evaluated to 20 mm with respect to the uneven modes (Fig. 3).

## 2.6. Conclusions on the composite bridging effect

As a conclusion, the bridging effect induced by the composite is characterised by:

- A neglectible influence outside the vicinity of the fault because of its low mass and low bending stiffness
- A great influence inside the active length located on both sides of the notch

So, the effect of the composite strengthening can be viewed as a longitudinal stiffness located in the vicinity of the crack and can be modeled by the approach formulated in Ovigne, Massenzio, Jacquelin, Hamelin (2002). This analytical model is implemented in the calculation of the active length.

## 3. Modeling of bridging force transfer on vicinity of the crack

### 3.1. Modeling of a beam with open cracks and external strengthening

The model is presented in further detail in Ovigne, Massenzio, Jacquelin, Hamelin (2002). It is based on the assembly of beam elements with interconnecting conditions resulting in the transfer matrix of the cracked section with external strengthening (Fig. 4). The effect of the open crack is taken into account according to stress concentration around the crack tip. So, a rotation stiffness  $k_{crack}^{\theta}$  of the cracked section is derived.

The longitudinal stiffness of the composite along its active length  $L_{active}$  is denoted as  $k_{repair}$  and is given by:

$$k_{repair} = \frac{E_{compo} S_{compo}}{L_{active}} \quad (1)$$

The cracked section with external strengthening is modeled by an elastic hinge located at the upper side of the beam. The rotation stiffness  $k_{hinge}^{\theta}$  given by:

$$k_{hinge}^{\theta} = k_{crack}^{\theta} + k_{repair}^{\theta} \quad (2)$$

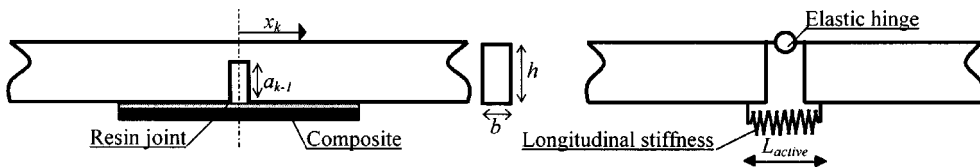


Fig. 4 External strengthening of a cracked section

where the rotation stiffness due to the composite is:

$$k_{repair}^{\theta} = h^2 k_{repair} \quad (3)$$

Then, the resulting flexibility associated with the rotation discontinuity is given by:

$$\overline{C}_{22} = \frac{1}{k_{hinge}^{\theta}} \quad (4)$$

The transfer matrix of the notched section with composite is then:

$$\begin{bmatrix} v \\ \theta \\ P \\ M \end{bmatrix}_{right}^{k-1} = \begin{bmatrix} 1 & 0 & 0 & 0 \\ 0 & 1 & 0 & \overline{C}_{22} \\ 0 & 0 & -1 & 0 \\ 0 & 0 & 0 & -1 \end{bmatrix}^k \begin{bmatrix} v \\ \theta \\ P \\ M \end{bmatrix}_{left}^k \quad (5)$$

The natural frequencies and mode shapes of the entire beam are calculated from the assembly of all the beam elements and each open crack with composite bridging. The beam elements are described by the Timoshenko theory where the transverse displacement  $v(x, t)$  and the section rotation  $\theta(x, t)$  are used. Separating time and space variables gives:

$$v(x, t) = v(x) e^{i\omega t} \quad (6)$$

$$\theta(x, t) = \theta(x) e^{i\omega t} \quad (7)$$

According to the governing equations of the beam element, the displacement magnitudes can be written as:

$$v(x) = \sum_{j=1}^4 A_j^k e^{p_j x} \quad (8)$$

$$\theta(x) = \sum_{j=1}^4 \left( p_j + \frac{m\omega^2}{p_j k A_{beam} G_{beam}} \right) A_j^k e^{p_j x} \quad (9)$$

And the shear force  $P$  and bending moment  $M$  magnitudes can then be expressed as:

$$P(x) = \sum_{j=1}^4 \frac{m\omega^2}{p_j} A_j^k e^{p_j x} \quad (10)$$

$$M(x) = \sum_{j=1}^4 EI \left( p_j^2 + \frac{m\omega^2}{k A_{beam} G_{beam}} \right) A_j^k e^{p_j x} \quad (11)$$

where  $p_j$  ( $j = 1$  to  $4$ ) are the four wave numbers derived from the characteristic polynom associated with the four degree equation of motion of a Timoshenko beam when expressions Eqs. (6) and (7)

are taken into account.  $A_j^k$  are constants that can be determined considering the assembly.

The assembly is devised for a beam with  $N$  notches. The four boundary conditions in terms of forces and displacements at each side of the entire beam in free-free conditions are added. It leads to a  $4(N + 1) \times 4(N + 1)$  system in terms of  $A_j^k$  coefficients Eq. (12).

$$\begin{bmatrix} \text{Mat} \\ \text{size } 4(N + 1) \times 4(N + 1) \end{bmatrix} \begin{bmatrix} A_1^1 \\ A_2^1 \\ \cdot \\ \cdot \\ A_3^{N+1} \\ A_4^{N+1} \end{bmatrix} = [0] \quad (12)$$

The natural pulsation  $\omega$  of the entire beam set the determinant of the matrix  $[Mat]$  equal to zero

$$\text{Det}[Mat](\omega) = 0 \quad (13)$$

For a given pulsation, the  $A_j^k$  coefficients vector in Eq. (12) is computed as a function of one arbitrary  $A_j^k$  coefficient and the mode shape is computed with Eq. (8).

### 3.2. Shear stress mode shapes inside the resin joint

The anchorage of a composite plate and the force transfer within a resin interface have already been studied (Bizindavyi and Neale 1999), (Chajes and Finch 1996). The analysis of the shear stress inside the adhesive layer has been studied by Täljsten (1997) for the static problem of peeling failure that can be encountered for beams with external composite strengthening. The Täljsten model is extended here to the modal problem of the bridging force transfer on each side of a crack so as to obtain a stress mode shape of the shearing inside the resin joint.

In the vicinity of the notch, the shear stress inside the resin joint is due to the relative displacements between the beam and the composite. It can be expressed as:

$$\tau(x) = \frac{G}{e}(u_{compo}(x) - u_{beam}(x)) \quad (14)$$

And then,

$$\frac{d\tau(x)}{dx} = \frac{G}{e}(\varepsilon_{compo}(x) - \varepsilon_{beam}(x)) \quad (15)$$

The composite is subjected to tensile loading then:

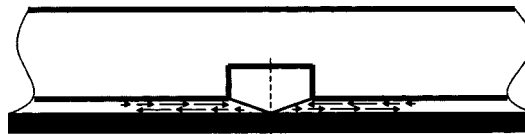


Fig. 5 Shear stress in the resin joint

$$\varepsilon_{compo}(x) = \frac{N_{compo}(x)}{E_{compo}A_{compo}} \quad (16)$$

The beam is subjected to bending:

$$\varepsilon_{compo}(x) = \frac{M(x)h}{2E_{beam}I_{beam}} \quad (17)$$

Eqs. (15), (16), (17) lead to

$$\frac{d^2 \tau(x)}{dx^2} = \frac{G}{e} \left( \frac{1}{E_{compo}A_{compo}} \frac{dN_{compo}(x)}{dx} - \frac{h}{2E_{beam}I_{beam}} \frac{dN_{beam}(x)}{dx} \right) \quad (18)$$

The equilibrium of the composite plate leads to:

$$\frac{dN_{compo}(x)}{dx} = \tau(x)b \quad (19)$$

$$\frac{dM(x)}{dx} = P(x) - b \frac{h}{2} \tau(x) \quad (20)$$

where  $v(x)$  and  $P(x)$  are given by Eqs. (8) and (10). Then, a second order differential equation in term of shear stress is obtained

$$\frac{d^2 \tau(x)}{dx^2} - \lambda^2 \tau(x) = \frac{-G_{beam}h}{2eE_{beam}I_{beamj=1}} \sum_{j=1}^4 \frac{m\omega^2}{p_j} A_j^k e^{p_j x} \quad (21)$$

where:

$$\lambda^2 = \frac{Gb}{e} \left( \frac{1}{E_{compo}A_{compo}} + \frac{h^2}{4E_{beam}I_{beam}} \right) \quad (22)$$

### 3.2.1. Boundary conditions

The shear stress is maximal at the cracked section. Its value is computed by considering the relative displacements of the notch lips.

$$\tau(0) = \frac{G}{e} (u_{compo}(0) - u_{beam}(0)) \quad (23)$$

For the composite:

$$u_{compo}(0) = 0 \quad (24)$$

For the beam element

$$u_{beam}(0) = \frac{h}{2} \theta_{beam}(0) \quad (25)$$

$\theta(x)$  is given in Eq. (9), and then:

$$u_{beam}(0) = \frac{h}{2} \sum_{j=1}^4 \left( p_j + \frac{m\omega^2}{p_j k A_{beam} G_{beam}} \right) A_j^k \quad (26)$$

Substituting Eqs. (24) and (26) in Eq. (23) leads to:

$$\tau(0) = -\frac{Gh}{e} \sum_{j=1}^4 \left( p_j + \frac{m\omega^2}{p_j k A_{beam} G_{beam}} \right) A_j^k \quad (27)$$

Furthermore, outside the active length, the bridging force is transferred to the beam element and then the shear stress is null:

$$\tau(L^k) = 0 \quad (28)$$

### 3.2.2. Solving

The solution to the homogeneous equation associated with Eq. (21) is:

$$\tau_1(x) = \varphi_1 e^{\lambda x} + \varphi_2 e^{-\lambda x} \quad (29)$$

Where  $\varphi_1$  and  $\varphi_2$  are constants. A particular solution to the non-homogeneous Eq. (21) can be found of the form:

$$\tau_2(x) = \sum_{j=1}^4 \psi_j e^{p_j x} \quad (30)$$

Where  $\psi_j$  for  $j = 1$  to 4 are constants expressed as:

$$\psi_j = \frac{1}{p_j^2 - \lambda^2} \left( \frac{-G_{beam} h}{2e E_{beam} I_{beam}} \frac{m\omega^2}{p_j} A_j^k \right) \quad (31)$$

Applying the boundary conditions Eqs. (27), (28) leads to:

$$\varphi_1 = \frac{1}{(e^{\lambda L} - e^{-\lambda L})} \left[ \frac{G_{re} \sin h}{2e} e^{-\lambda L} \sum_{j=1}^4 \left( p_j + \frac{m\omega^2}{p_j k A_{beam} G_{beam}} \right) A_j^k + \sum_{j=1}^4 \psi_j (e^{-\lambda L} - e^{p_j L}) \right] \quad (32)$$

and

$$\varphi_2 = \frac{-Gh}{2e} \sum_{j=1}^4 \left( p_j + \frac{m\omega^2}{p_j k A_{beam} G_{beam}} \right) A_j^k - \sum_{j=1}^4 \psi_j - \varphi_1 \quad (33)$$

Then, the general solution to Eq. (21) is:

$$\tau(x) = \tau_1(x) + \tau_2(x) \quad (34)$$

## 4. Experimental validation

### 4.1. Eigen frequencies of a cracked beam with composite strengthening

The 765 mm long steel beam with 3 notches is tested with 3 reinforcement configurations:



Table 3 Natural frequencies (Hz). CFRP on all notches

| Mode number | Experiment | Model | Error (%) |
|-------------|------------|-------|-----------|
| 1           | 293        | 291   | 0.7       |
| 2           | 835        | 833   | 0.3       |
| 3           | 1479       | 1471  | 0.5       |
| 4           | 2895       | 2920  | 0.9       |
| 5           | 4010       | 3969  | 1.0       |

Table 4 Natural frequencies (Hz). CFRP on the central and one extremal notches

| Mode number | Experiment | Model | Error (%) |
|-------------|------------|-------|-----------|
| 1           | 286        | 286   | 0.0       |
| 2           | 779        | 784   | 0.7       |
| 3           | 1406       | 1410  | 0.3       |
| 4           | 2876       | 2904  | 1.0       |
| 5           | 3974       | 3964  | 0.3       |

Table 5 Natural frequencies (Hz). CFRP on the central notch

| Mode number | Experiment | Model | Error (%) |
|-------------|------------|-------|-----------|
| 1           | 281        | 280   | 0.1       |
| 2           | 741        | 743   | 0.3       |
| 3           | 1341       | 1343  | 0.1       |
| 4           | 2845       | 2886  | 1.5       |
| 5           | 3951       | 3959  | 0.2       |

- The 3 notches are bridged (Table 3)
- Only the extrem notches are bridged (Table 4)
- Only one extreme notch is bridged (Table 5)

The experimental results are compared to those obtained by the model. The analytical modeling takes into account the active length of the composite (Fig. 3). The results point out the ability of the model to predict the natural frequencies of the beam with less than 2% of error for the five first bending modes.

#### 4.2. Shear stress mode shapes inside the resin joint

The experimentally validated analytical modeling (§ 4.1), is then used to determine the shear stress mode shapes inside the resin joint on the third beam element associated with the beam with 3 notches and CFRP on the central one. For this element, the axial coordinate  $x_3$  varies from 0 up to 0.191 m.

The shear stress  $\tau(x_3)$  calculation involves Eqs. (14) to (34) with all the parameters needed obtained from analytical modeling. Once the shear stress is computed along the span, the stress mode shape is normalized by dividing  $\tau(x_3)$  by  $\tau(0)$ . The evolution of  $\tau(x_3)$ , for the three first uneven bending modes (Figs. 6, 7 and 8), is compared to this of the relative variations of the eigen frequency ( $\Delta f_i/f_i$ ) presented

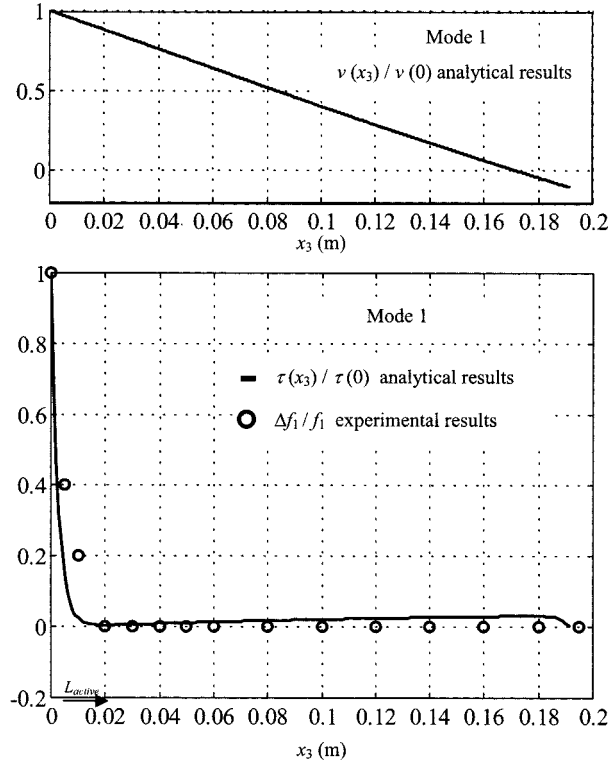


Fig. 6 First shear stress mode shape, mode shape, frequency drop

in (Fig. 3). When  $\Delta f_i / f_i(x_3)$  is null, it means that  $x_3$  is higher than the active length or, as can be seen for higher modes, the curvature of the element helps the composite to be anchored on the beam (Figs. (7) and (8)).

The mode shapes are needed to point out the influence of the curvature of the beam element on the evolution of shear stress.

The results concerning  $\tau(x_3)$  show that the shear stress sharply decreases from the tip of the beam element up to a point that corresponds to the half of the active length. An approximately 20 mm long active length can be observed in (Figs. 6, 7 and 8). These results are in agreement with experimental results concerning the frequency drop obtained when the composite is progressively cut up around the notch. The shear stress is influenced by the beam element curvature. This is clearly shown on Fig. 8. For  $x_3 = 0.11$  m,  $\tau(x_3)$  reverses sign, as the transverse displacement  $v(x_3)$  is quasi maximum and in the same time,  $\theta(x_3)$  reverses sign (the small gap is due to the presence of the notch that disturbs the shear stress along the beam element). When  $\tau(x_3)$  is null, the composite is anchored. So in Fig. 8, the composite between  $x_3 = 0.11$  m and  $x_3 = 0.191$  m is anchored and is not disturbed by the notch and is independent from the composite located between  $x_3 = 0$  m and  $x_3 = 0.11$  m and acts as a composite bonded on an uncracked beam. Then,  $\tau(x_3)$  is maximal when  $v(x_3)$  is null. As shown in (§ 2.3) this portion of composite has no significant influence on the frequency of the beam and then the frequency drop can be neglected when the composite of this zone is cut up (Fig. 8). In that zone, the remaining shear stress is only due to the beam element curvature.

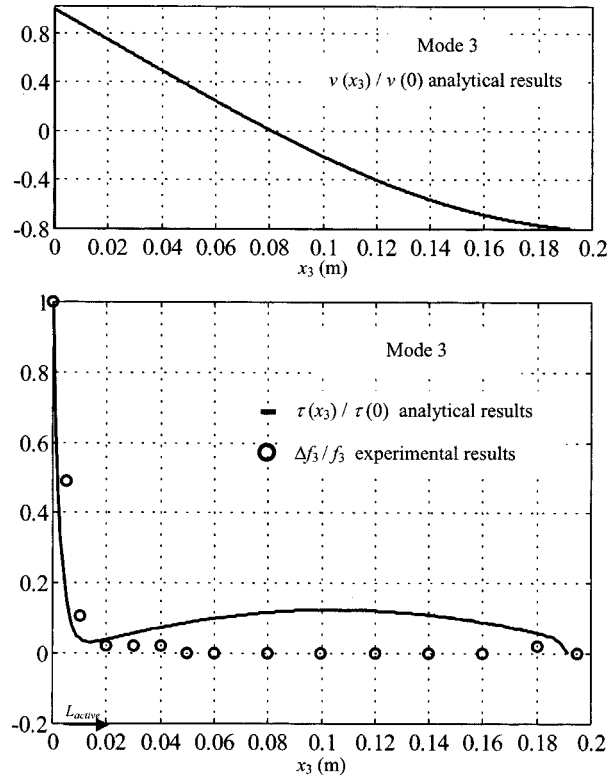


Fig. 7 Third shear stress mode shape, mode shape, frequency drop

## 5. Discussion

The primary parameter associated with the influence of the composite strengthening is the active length. This parameter is greatly influenced by the resin joint thickness  $e$ . Fig. 9 presents the evolution of  $\tau(x_3)$  for various values of resin joint thicknesses and for the first mode. When  $e$  increases, the active length of the composite increases too and the frequency decreases. Then in order to study the influence of  $e$  on a given mode, an iterative calculation is needed. First, the active length is evaluated for a frequency  $f_1$  of 291 Hz (Table 3), then it is used to compute a new frequency  $f_1'$ . Then, a new active length is computed for a frequency of  $f_1'$  and so on. The results convergence is obtained with few iterations for a precision of 0.1 Hz.

Fig. 9 shows that the composite active length is doubled when the thickness of the resin joint increases in the range of  $0.8 \cdot 10^{-4}$  m to  $3 \cdot 10^{-4}$  m, corresponding to the practical values that can be observed.

## 6. Conclusions

The first step of this study has shown that a carbon epoxy external strengthening can significantly influence the modal scheme of a cracked beam. The longitudinal stiffness of the composite intervenes so as to limit the relative displacements of the crack lips, resulting in an enhancement of the stiffness of

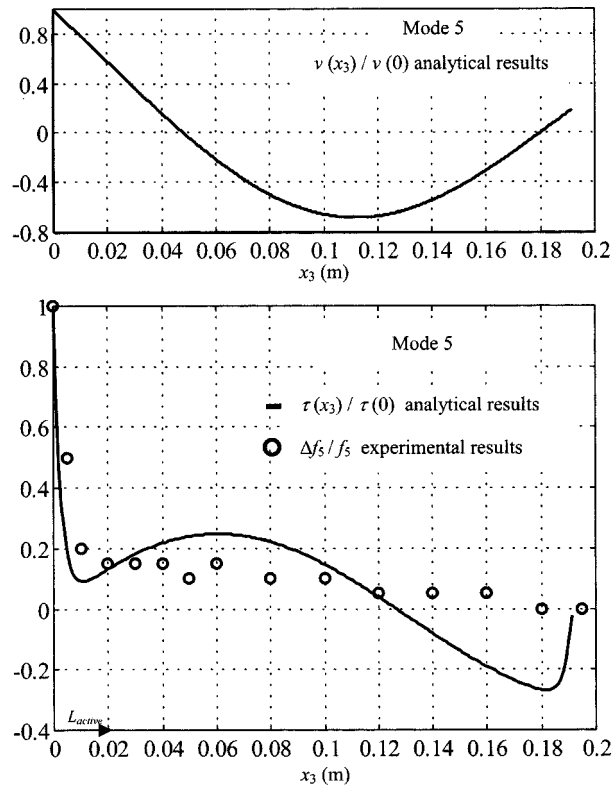


Fig. 8 Fifth shear stress mode shape, mode shape, frequency drop

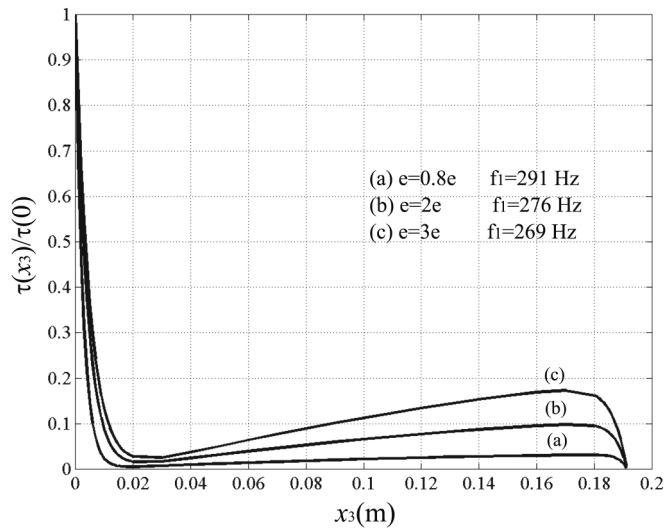


Fig. 9 Influence of the resin joint thickness on the composite active length

the cracked section. This effect, called crack bridging, implies an active length of the composite. This parameter derives from the transfer mechanism of the bridging force on both sides of the crack and can

be experimentally evaluated by the procedure described in this paper. Furthermore, the low mass of the composite material does not modify the mass terms of the problem and the influence of the composite can be consequently neglected outside the vicinity of the cracks.

As a consequence, a cracked beam with composite strengthening can be modeled by an assembly of beam elements with interconnecting conditions described in Ovigne, Massenzio, Jacquelin, Hamelin (2002) in which active length of the composite is taken into account. Then, a modal extension of Täljstens model is proposed in order to compute shear stress mode shapes of the resin. The stress mode shapes are used to evaluate the active length of the composite.

Finally, the analytical model is experimentally validated under specific specimens allowing the control of both the leading assumptions of the modeling and of the crack geometries. The validation for a steel beam with three notches for various strengthening configurations showed good agreement between the experimental natural frequencies and the experimental ones (2% error). The analytical evaluation of the composite active length based on shear stress mode shapes determination showed good agreement with the experimental value obtained from the procedure developed.

The prediction of the eigen frequencies of cracked reinforced concrete beams with composite strengthening will be undertaken soon.

## References

- Bizindavyi, L., Neale, K.W. (1999), "Transfer lengths and bond strength for composites bonded to concrete", *Journal of Composites for Construction*, **3**(4), 153-160.
- Chajes, M.J., Finch, W.W.Jr. (1996), "Bond and force transfer of composite material plates bonded to concrete", *ACI Structural Journal*, **93**(2), 208-217.
- Meier, U., Deuring, M., Meier, H., Schwegler, G. (1992), "Strengthening of structures with CFRP laminates: research and applications in Switzerland", *Proceedings of ACMBSI*, Canada, 243-251.
- Ovigne, P.-A., Massenzio, M., Jacquelin, E., Hamelin, P. (2002), "Analytical model for the prediction of the eigen modes of a beam with open cracks and external strengthening", *Int. J. of Structural Engineering and Mechanics*, Provisionally Accepted.
- Triantafillou, T. (1998), "Shear strengthening of reinforced concrete beams using epoxy-bonded FRP", *ACI Structural Journal*, **95**, 107-115
- Täljsten, B. (1997), "Defining anchor lengths of steel and CFRP plates bonded to concrete", *Int. J. of Adhesives*, **17**(4).
- Täljsten, B. (1997), "Strengthening of beams by plate bonding", *J. of Materials in Civil Engineering*, **9**(4), 206-212.

## Notation

|                |   |
|----------------|---|
| $A$            | Beam cross sectional area                                 |
| $A_j^k$        | Coefficients associated with $v(x)$                       |
| $a, a_k$       | Notch length, notch length of the $k^{th}$ notch          |
| $B_j^k$        | Coefficients associated with $\theta(x)$                  |
| $b$            | Beam width  |
| $C_{ij}$       | Flexibility matrix term                                   |
| $C_j^k$        | Coefficients associated with $P$                          |
| $e$            | Thickness of the resin joint                              |
| $E, E_{compo}$ | Young modulus and longitudinal Young modulus of composite |

|                                       |  |
|---------------------------------------|--|
| $f_i$                                 | Natural frequency associated with the mode $i$                                     |
| $G$                                   | Shear modulus  |
| $h$                                   | Beam height  |
| $I$                                   | Beam inertia   |
| $K_{IM}, K_{IP}$                      | Strain intensity factor associated with $M$ and to $P$ for the first opening mode  |
| $K_{IIP}$                             | Strain intensity factor associated with $P$ for the second opening mode            |
| $k$                                   | Shear factor   |
| $k_{hinge}^\theta, k_{repair}^\theta$ | Rotation stiffness of the elastic hinge, external strengthening rotation stiffness |
| $k_{repair}$                          | External longitudinal stiffness  |
| $L_{active}$                          | Composite active length  |
| $M$                                   | Bending moment   |
| $m$                                   | Mass   |
| $P$                                   | Shear force  |
| $P_i$                                 | Generalized force $P_1 = M$ and $P_2 = P$  |
| $p_j$                                 | Wave number  |
| $S_{compo}$                           | Composite cross sectional area   |
| $t$                                   | Time   |
| $v(x), v(x, t)$                       | Transverse displacement amplitude and transverse displacement                      |
| $W_{notch}$                           | Strain energy associated with a notch  |
| $x_k$                                 | Axial coordinate associated with the $k^{th}$ beam element                         |
| $\beta$                               | Shear rotation   |
| $\theta(x), \theta(x, t)$             | Global rotation amplitude and global rotation                                      |
| $\nu$                                 | Poisson ratio  |
| $\omega$                              | Natural angular frequency  |
| $\zeta$                               | Non-dimensional parameter associated with $a$                                      |
| CC                                    |  |